Research Article | Vol. 30, No. 17 / 15 Aug 2022 / Optics Express 31171

Optics EXPRESS

X-ray pulse generation with ultra-fast flipping of its orbital angular momentum

J. MORGAN[1,*] AND B. W. J. MCNEIL[2,3]

[1] SLAC National Accelerator Laboratory, Menlo Park, California, 94025, USA
[2] University of Strathclyde (SUPA), Glasgow G4 0NG, United Kingdom
[3] Cockcroft Institute, Warrington, WA4 4AD, United Kingdom
[*] jmorgan@slac.stanford.edu

Abstract: A method to temporally tailor the properties of X-ray radiation carrying Orbital Angular Momentum (OAM) is presented. In simulations, an electron beam is prepared with a temporally modulated micro-bunching structure which, when radiating at the second harmonic in a helical undulator, generates OAM light with a corresponding temporally modulated intensity. This method is shown to generate attosecond pulse trains of OAM light without the need for any additional external optics, making the wavelength range tunable. In addition to the OAM pulse train, the method can be adapted to generate radiation where the handedness of the OAM mode may also be temporally modulated (flipped).

1. Introduction

Light-matter interactions play an important role in our understanding of material interactions across most of science, from how viruses function to the properties of matter at the centre of gas giant planets. The material properties that can be observed depend critically upon the form of the light used: wavelength, intensity, temporal duration etc. Much research is therefore devoted to improving upon, or developing new forms of light, that can access previously unobserved material properties.

Increasing attention is being given to light with helical wave-fronts, as its transverse phase rotation means the light carries orbital angular momentum (OAM). This OAM is distinct from the spin momentum of the light and can be significantly greater, allowing another dimension of light-matter interactions to be explored and utilised. Allen *et al.* [1] was first to recognise that OAM is a property belonging to light with an azimuthal phase dependence given by $\exp i\ell\phi$, where ϕ is the azimuthal angle and ℓ the mode index. Since publication of this seminal paper in 1992, there has been significant research interest in the scientific applications of this light which has benefited numerous fields [2] such as imaging [3,4] and communication [5]. As OAM can be exchanged with atoms and molecules, there has also been great interest in the study of OAM light with matter [6–10]. This is being further developed by investigating new methods to generate OAM light pulses that can interact with matter at its fundamental spatial (X-ray wavelengths) and temporal (attosecond) scales [11–14].

There has been specific interest in the generation of pulses of OAM light at XUV and X-ray wavelengths due to predicted experimental applications [15,16]. To meet this need, short individual pulses and trains of pulses have been generated at XUV using high harmonic generation [17–20]. Although these methods are predicted to work into the soft X-ray, this is yet to be demonstrated. OAM light can be generated by manipulating the phase profile of Gaussian beams with $l = 0$ using optical elements which convert the light phase. These require precise fabrication which can be particularly challenging at shorter wavelengths, although elements which work at XUV and X-ray wavelengths are becoming increasingly available [21]. However, these optical

#470503 https://doi.org/10.1364/OE.470503
Journal © 2022 Received 13 Jul 2022; accepted 14 Jul 2022; published 10 Aug 2022

Optics EXPRESS

elements are not tuneable, so different elements are required at different wavelengths, and are susceptible to damage at the high intensities made possible by FELs. Such conventional optical elements can also pose a barrier to the rate at which the OAM mode of the light can be controlled. Routine OAM switching optics, such as spatial light modulators, only achieve a mode switching rate in the kHz range, although this could possibly be improved on with more complex techniques.

In recent developments at short wavelengths, a temporal variation in the OAM of a light beam (a 'self-torqued' beam) has been achieved using harmonic generation [22] and opens up another new branch of potential applications.

Free Electron Lasers (FELs) provide a method for generating intense OAM light without the need for additional optical elements. There has been significant progress in the generation of light with OAM in a FEL including experimental demonstration [23,24] and the proposed combination of OAM modes to generate Poincaré X-ray beams [25]. However, current FEL studies have not yet considered the detailed control of the temporal properties of the OAM light.

In this article, a new method is proposed to use a FEL to generate high power, X-ray OAM light with attosecond intensity modulation. The approach uses a FEL 'afterburner' configuration [26]. This consists of a main FEL lasing section that first develops a strongly modulated electron beam micro-bunching which is then injected into the helical undulator afterburner where the attosecond timescale, temporally modulated OAM light is generated. A small modification to this approach, the addition of a second afterburner undulator, allows the generation of light pulses which alternate between $l = \pm 1$ OAM modes, again at attosecond timescales. The alternation of OAM light at such fast timescales and short wavelengths would be the first demonstration of such output.

2. Orbital angular momentum from relativistic electron beams

OAM was first shown to be carried by the harmonic radiation emitted from electrons propagating in a spiral path through a helical undulator [27,28]. The light may be described via Gauss-Laguerre modes can be characterised by the OAM index:

$$\ell = \pm(h - 1), \tag{1}$$

where h is the harmonic number of the radiation and the mode index ℓ, is sign dependent upon the handedness of the undulator. This theoretical work was subsequently experimentally corroborated with OAM demonstrated to be carried by both incoherent and coherent undulator radiation [24,29]. Other methods have been proposed to generate OAM light with relativistic electron beams. Some of these methods do not require emission at the harmonics of the emitting undulator [23,30], while other methods simply filter out harmonic radiation from the helical undulator, which contains the OAM emission, by using optical filters. Such filters, however, have very limited tunability and can be fragile at the high intensities generated by an FEL.

Here, a FEL afterburner arrangement is used [29] in which an energy modulated electron beam is used. An FEL amplifier then bunches the electron beam before it is propagated into a downstream helical undulator, the afterburner, where the OAM light emission takes place. The pre-prepared electron bunching is at the second harmonic of the helical undulator afterburner resonance and generates the coherent harmonic emission of radiation which carries the desired OAM. This energy-modulation – FEL bunching – afterburner scheme is a relatively flexible arrangement, which does not require any optical elements to filter or change optical modes, and forms the basis of several, more advanced FEL methods being adopted at FEL facilities and designs [31,32].

3. Generation of light pulses with alternating OAM

A method is now proposed to generate a train of ultra-short light pulses with alternating OAM of $\ell = +1, -1, +1, \ldots$. The method uses a similar setup as the 2nd harmonic helical undulator OAM

Optics EXPRESS

afterburner [33], but with an electron beam prepared so that its micro-bunching is modulated into a periodic comb structure. This can be obtained by using an energy modulated electron beam in the first FEL amplifier that induces the electron micro-bunching. When emitting in a short helical afterburner undulator, the modulated micro-bunching of the electron beam causes emission of a train of coherent OAM light pulses spaced at the modulation frequency, in a similar way to that described in [34]. If a second OAM afterburner undulator, with the same tuning but opposite handedness as the first, is added, a second interweaving light pulse train can be superimposed so that the final light generated alternates between OAM $\ell = \pm 1$ mode pulses of approximately the same power.

3.1. Modulating the electron beam micro-bunching

Like many methods that have been proposed to extend the operational range of FELs, the following method uses an electron beam which has had its energy modulated at a wavelength λ_m, significantly greater than the final output radiation wavelength. Such a beam can be obtained in a relatively short, seeded FEL undulator called the 'modulator'. Many FEL facilities now incorporate, or propose to use, such modulators at the start of their FEL interaction region e.g. SwissFEL [35], FERMI [36] and FLASH [37] with the latter simulating modulated beam energies at wavelengths down to $\lambda_m = 50$ nm. Other facility design proposals have simulated energy modulations down to $\lambda_m = 12.4$ nm using HHG seed lasers [38]. In what follows, we use a modulation period of $\lambda_m = 100$ nm.

When a relativistic electron beam is prepared in a FEL modulator section with a sinusoidal energy modulation, $\gamma(t) = \gamma_0 + \gamma_m \cos(\omega_m t)$, the energy gradients about the mean energy γ_0 'spoil' the FEL interaction there. No seeding of the FEL is required and the process starts up from noise. If the modulation amplitude, γ_m, is sufficiently large, the only regions that develop any significant electron FEL micro-bunching are about the minima of the energy modulated beam [34]. Following a preparatory process in a FEL amplifier, the energy modulated electron beam then has regions of relatively high micro-bunching separated by the modulation period $\lambda_m = 2\pi/\omega_m$.

When the electron beam with this modulated electron micro-bunching structure is then propagated through a short OAM afterburner undulator module, the power of the coherent OAM light emitted then has the same modulation period of λ_m.

The modulation in the temporal power profile of the radiation corresponds to a frequency spectrum which is broader than the typical FEL output and is discretized into frequency modes. To examine the effect of this on OAM mode purity we first present analysis of the spectral output of a single undulator module. Following this, simulations of the method to generate pulse trains of OAM light, as well as pulse trains with alternating OAM, are presented.

3.2. Spontaneous emission spectrum of a single undulator module

To examine the OAM content of a helical undulator at the second harmonic, the far field radiation emitted by a single electron propagating in a helical undulator [33] is multiplied by the term $\exp(-\sigma_x^2\omega^2/c^2 \sin^2\theta)$, which captures the restriction imposed by the beam's transverse dimensions on the angle of emission θ. A Gaussian transverse profile is assumed, where σ_x is the rms beam radius. The radiation spectrum is then considered in terms of OAM content. Figure 1 plots the radiation spectrum decomposed into different OAM modes (as in [23]) for different numbers of undulator periods, N_u. An undulator parameter of a_u>1 is used, increasing the fractional power emitted into the $\ell = 1$ mode [33].

It can be seen that undulators with a lower number of periods N_u, have significant emission into the fundamental Gaussian mode with $\ell = 0$. For a long electron beam bunched uniformly at the second harmonic, the bunching picks out a narrow region of the FEL bandwidth about the

Optics EXPRESS

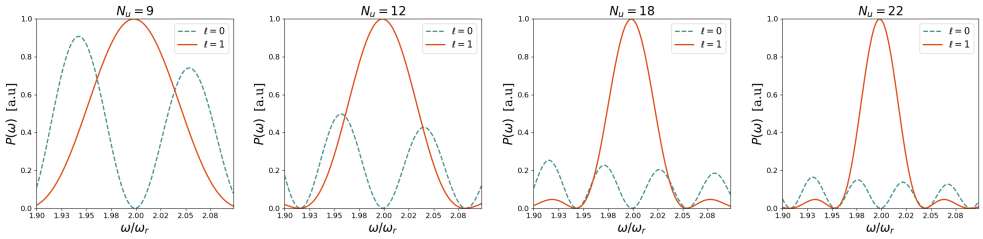

Fig. 1. Spectrum of helical undulator radiation for different number of undulator periods $N_u = 9, 12, 18, 22$ with $a_u = 2.634$, $\lambda_u = 3.9$cm, $\gamma = 7869$ and $\sigma_x = 26\mu$m.

peak of the $\ell = 1$ emission. There is therefore little emission into the Gaussian mode when the micro-bunching structure is not modulated as assumed in the simple OAM afterburner.

When the electron beam micro-bunching is modulated to have a comb structure, as described in Section 3.1, then radiation pulses are generated at the modulation period. For a small number of undulator periods N_u, it can be seen from Fig. 1 that a significant fraction of the power can be emitted off-resonance into the $\ell = 0$ mode. Increasing N_u both increases the relative fraction of power in the $\ell = 1$ mode, and decreases the bandwidth with FWHM spectral width of harmonic, h given by:

$$\Delta\omega_h = \frac{0.88}{hN_u}\omega_h(\theta), \tag{2}$$

where $\omega_h(\theta)$ is the peak of the spectrum.

4. Numerical simulations

Using the FEL simulation code Puffin [39,40], the generation of OAM pulse trains in the soft X-ray is demonstrated. Figure 2 shows a schematic of the layout used to generate two different types of pulse trains: a) each pulse has an OAM with index of $\ell = 1$; and b) the pulses have an OAM index that alternates between $\ell = \pm 1$.

The method is modeled using parameters inspired by the LCLS-II project at SLAC [41]. A 40 fs long electron beam is considered with a flat top beam current profile and current $I = 1$ kA. The energy is 4 GeV and the radius and emittance are $\sigma_x = 22$ μm and $\epsilon_{x,y} = 3.5$ mm − mrad respectively.

4.1. OAM pulse train generation

The electron beam is first prepared in a seeded undulator modulator to give it an energy modulation of amplitude $\gamma_m/\gamma_0 = 0.0014 \approx \rho$ (where ρ is the FEL parameter [42]) and period $\lambda_m = 100$ nm. This relatively long wavelength energy modulation is imposed as initial conditions on the electron beam without the need for simulations (detailed simulations have demonstrated it is relatively easy to achieve such modulation [43,44].)

The energy modulated electron beam is then micro-bunched in a planar undulator FEL amplifier with rms undulator parameter $\bar{a}_u = 1.72$, period $\lambda_u = 3.9$ cm and at the resonant wavelength $\lambda_r = 1.25$ nm. The micro-bunching at the resonant wavelength occurs at the minima of the energy modulations where the gain is greater. Figure 3 shows the bunching structure which has been established at the end of the FEL amplifier. The regions of the electron beam with high electron bunching will emit coherently in the afterburner so that a modulation in the electron bunching parameter leads to a corresponding modulation in the radiation intensity.

The first amplifier stage has a small reverse taper in the undulator parameter $\bar{a}_u$ [45]. This reduces the intensity of radiation emitted by the electrons without any significant reduction to the electron bunching at λ_r. In addition to using a reverse taper to suppress the radiation output from

Optics EXPRESS

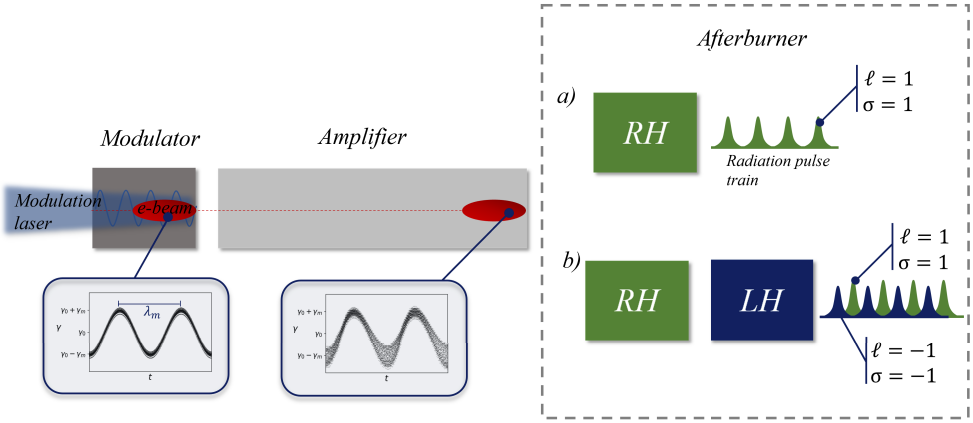

Fig. 2. The electron beam energy is modulated before injection into an amplifier undulator where the beam develops a micro-bunching structure. A pulse train of radiation carrying OAM radiation is then emitted in the short helical afterburner tuned to the second harmonic of the electron micro-bunching. In *a*) a single helical undulator afterburner will produce a single handed OAM pulse train, while in *b*) a second helical undulator with opposite handedness is added. The OAM pulse trains can be made to alternate spatially, resulting in the generation of OAM pulses that alternate in handedness between $\ell = \pm 1$.

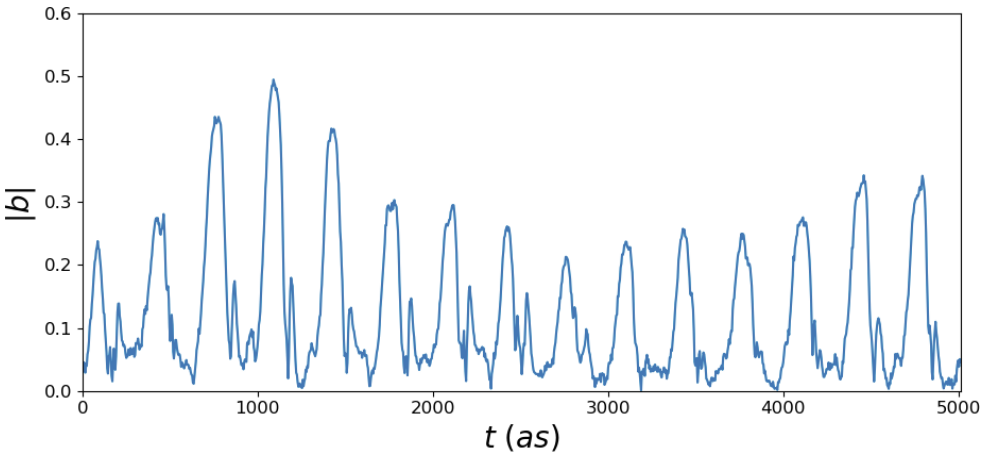

Fig. 3. Electron bunching parameter ($0<|b|<1$) as a function of relative time for a section of electron beam captured near the end of the FEL amplifier.

Optics EXPRESS

the modulator section, a small steering of the electron beam away from it before entry into the afterburner sections can also be used as described in [46]. In the simulations presented here, the steering of the electron beam is not modeled explicitly - the radiation generated in the modulator is simply removed before injection into the afterburner sections.

Following the preparation of the 4 GeV electron beam, with a micro-bunching at 1.25 nm modulated at $\lambda_m = 100$ nm, it is then injected into the afterburner section where the OAM output is generated. The first undulator module is a right-handed helical undulator with $\bar{a}_u = 2.634$, $\lambda_u = 3.9$ cm and $N_u = 20$. The fundamental resonant wavelength is then $\lambda_1 = 2.5$ nm, so that the electrons are micro-bunched at the 2nd harmonic. The relative propagation distance, or 'slippage', of a wavefront through the electrons is then $N_u\lambda_1 = \lambda_m/2$, one half of the electron beam modulation period.

In Fig. 4 it is seen that the modulated micro-bunching of the electron beam at the 2nd harmonic of resonant wavelength on the helical afterburner emits a pulse train of OAM light of mode $\ell = 1$ and wavelength $\lambda_{OAM} = 1.25$ nm. Each pulse has a FWHM pulse duration of $\tau \approx 167$ as, approximately 40 optical cycles corresponding to twice the number of helical undulator periods.

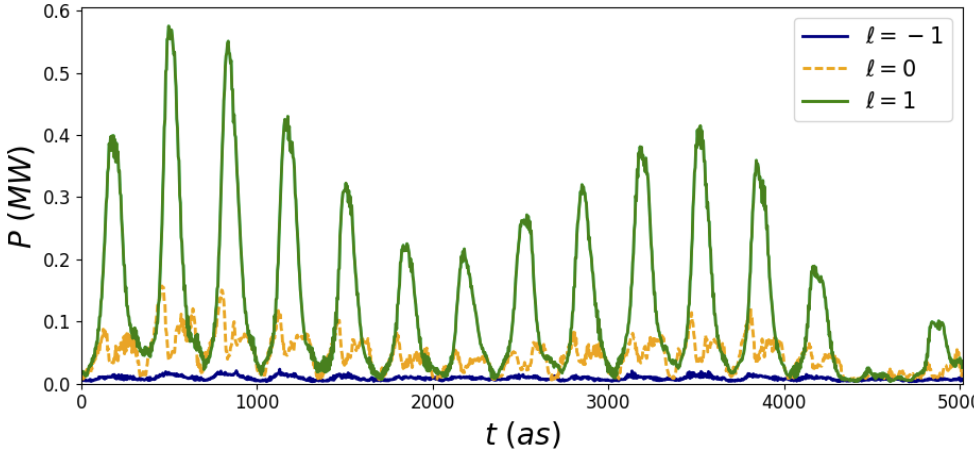

Fig. 4. Temporal plot of the radiation power output from the $\ell = 1$ helical afterburner decomposed into OAM modes. The radiation wavelength $\lambda_{OAM} \approx 1.25$ nm and the pulse FWHM durations are $\tau \approx 40\ \lambda_{OAM}/c = 167$ as.

It is seen that in addition to the OAM emission there is also some coherent emission into the $\ell = 0$ mode. This emission is expected due to the relatively short length of the afterburner undulators needed to produce short pulses as discussed in section 3.2. The length of the undulator is fixed to generate a specific pulse length.

We note that reducing the cross-sectional radius of the electron beam allows the radiation to be emitted into larger angles where power is directed into the single OAM mode. The coherent power of the harmonic radiation depends on electron beam radius according to relation [33], $P \propto \ln\left(\frac{1+4N^2}{4N^2}\right)$ where $N = k\sigma_x^2/L_u$ is the Fresnel number of the electron beam beam with $k = 2\pi/\lambda_{OAM}$, and L_u the length of the undulator. Hence, strong focusing of the electron beam to a smaller radius, by itself, could greatly improve the mode purity. However, strong focusing of the electron beam after the amplifier section would decrease, or even destroy, the beam micro-bunching. The electron beam transverse size is therefore limited by the requirements of the amplifier section, where the FEL interaction and transverse coherence would be negatively affected by a decreased beam size with resultant increased diffraction.

Optics EXPRESS

4.2. Time varying OAM

A left-handed helical undulator is now added to the right-handed afterburner (see Fig. 2 b)) with the same length and tuning. Previous versions of this crossed undulator configuration have been used to enable polarization control at the fundamental [47,48], spatially varying polarization [49] and the generation of Poincaré beams [25]. Recently, crossed undulators have been proposed as a method to modulate the polarization much in the same way we alternate the OAM here [50,51].

The additional undulator emits a second pulse train with OAM mode $\ell = -1$. The slippage in the first undulator means that this $\ell = -1$ pulse train is shifted relative to the first by half a modulation period. The combined pulse train from the two afterburners then consists of a sequence of pulses that alternate between $\ell = 1$ left-handed circularly polarized light and $\ell = -1$ right-handed circularly polarized light. Figure 5 shows the power radiation pulse train after the second afterburner decomposed into the different OAM modes and the corresponding normalized Stokes parameter s_3. The individual pulses have the same pulse length, $\tau_p = 167$ as, as before. The time between pulse peaks is also 167 as, corresponding to a switching rate of 6 PHz.

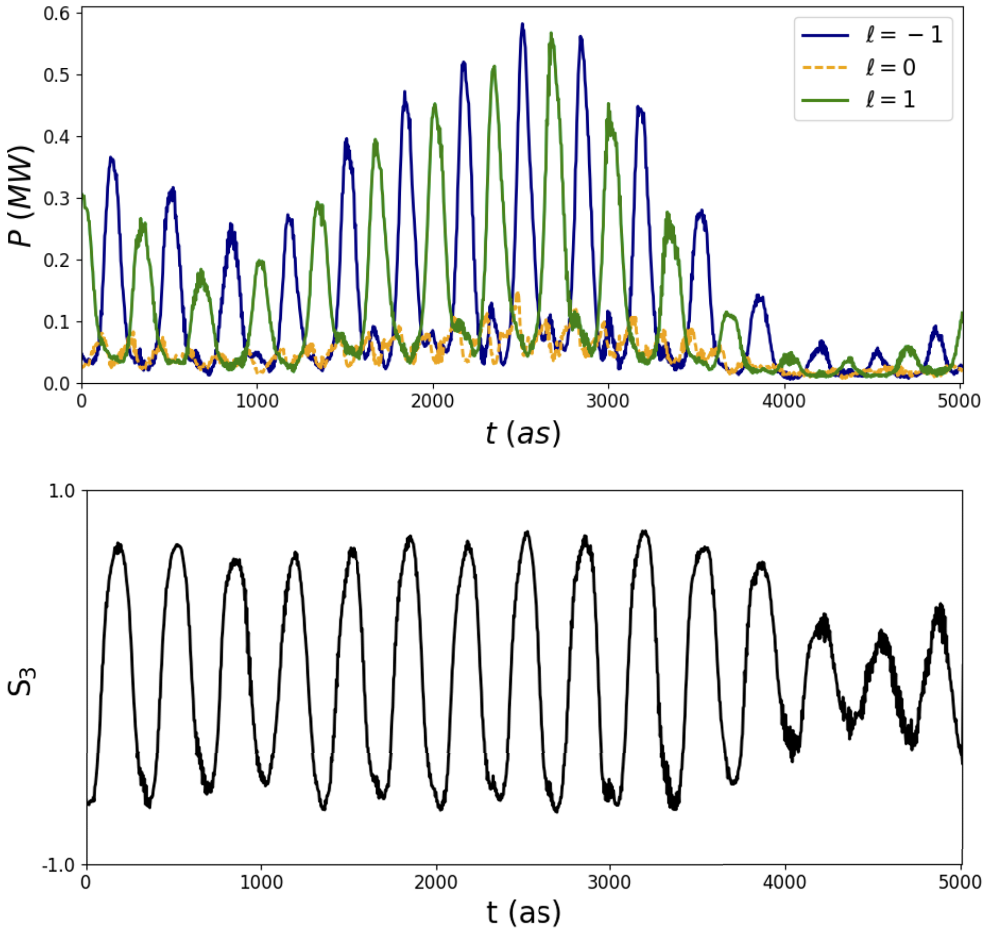

Fig. 5. Top: Power Vs relative time at the end of the afterburner for FEL radiation decomposed into OAM different modes. Bottom: normalized Stokes parameter s_3 vs time. Note that s_3 does not oscillate perfectly between ±1 due to the presence of some power in the other modes with other polarizations.

Optics EXPRESS

The intensity profile and phase of the radiation of two consecutive pulses with modes $\ell = 1$ and $\ell = -1$ is shown in Fig. 6. The intensity (averaged over a single spike) shows the typical OAM 'doughnut' profile in the transverse plane. The phase of the radiation is captured near the intensity peaks of two neighboring radiation spikes. There is a clear azimuthal phase distribution which changes handedness in the 167 as interval between snapshots.

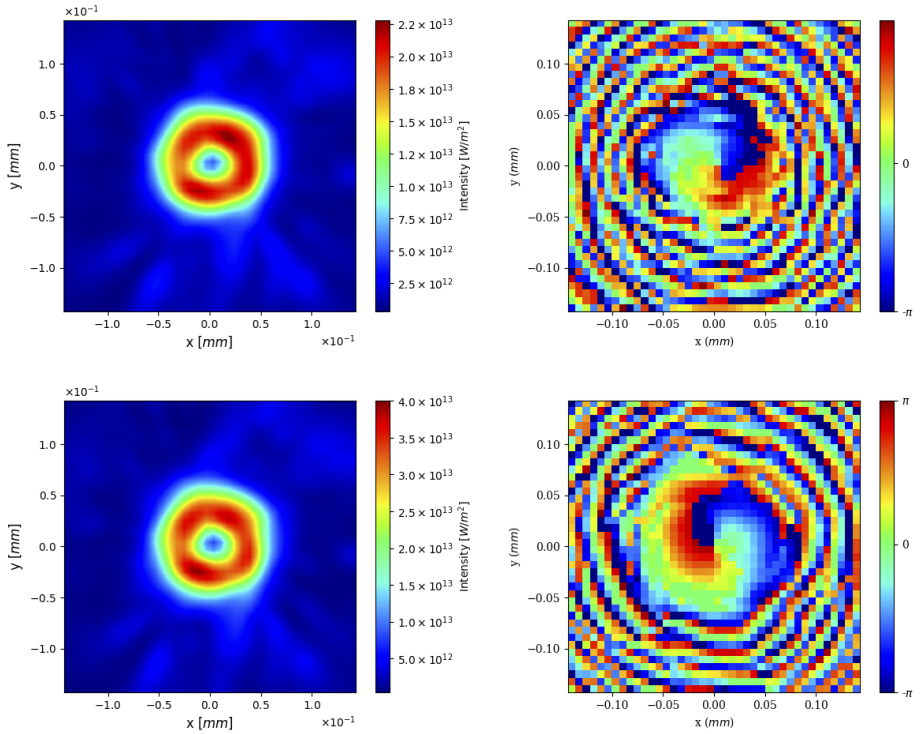

Fig. 6. Left: Pulse intensity averaged over a single pulse and Right: instantaneous phase for the pulses at relative times $t = 2516$ as (top) and $t = 2683$ as (bottom) in Fig. 5.

Also included in the Fig. 5 is the normalized Stokes parameter for circular polarization

$$s_3 = \frac{|E_R|^2 - |E_L|^2}{|E_R|^2 + |E_L|^2}, \tag{3}$$

The polarization of the light alternates along with the OAM mode. This then provides an interesting case as the polarization rotates in the same direction as the OAM. The total angular momentum contribution from the OAM plus the spin momentum add and therefore the pulse train alternates between total angular momentum $\pm 2\hbar$. We also note that tuning one of the afterburner undulators so that emission is at the fundamental frequency will produce pulses with no OAM. This $\ell = 0$ mode will be emitted from helical and planar undulators and thus a variety of OAM and spin combinations are available.

If OAM pulses with only one polarization are required, a linear polarizer which will filter out one linear polarization component may be a solution. Filtering out linear polarization corresponding to the polarization of the amplifying FEL section would also help ensure light emitted in this section does not interfere with the final pulse train delivered to experiment.

Optics EXPRESS

5. Conclusion

Ultra-fast manipulation of the temporal properties of FEL generated OAM light have been proposed and simulated for the first time. The method can be used to generate a pulse train of light carrying OAM and also alternate the handedness of the OAM at ultra-fast timescales. It was shown that the temporal profile of OAM radiation emitted from electrons can be controlled by tailoring the structure of micro-bunching in the electron beam. In addition, since the handedness of the OAM is determined by the magnetic undulator and not external optics, FELs are uniquely positioned to offer ultra-fast flipping of OAM handedness at X-ray wavelengths.

Funding. U.S. Department of Energy (Award No. 2021-SLAC-100732, Contract No. DE-AC02-76SF00515); Science and Technology Facilities Council (Agreement Number 4163192 Release#3); Engineering and Physical Sciences Research Council (Grant EP/M011607/1, Grant EP/K000586/1); John von Neumann Institute for Computing (NIC) on JUROPA at Jülich Supercomputing Centre (JSC) (project HHH20).

Acknowledgments. The authors would like to thank Erik Hemsing and Robert Cameron for providing helpful comments in the preparation of this paper.

Disclosures. The authors declare that there are no conflicts of interest related to this article.

Data availability. Data underlying the results presented in this paper are not publicly available at this time but may be obtained from the authors upon reasonable request.

References

1. L. Allen, M. W. Beijersbergen, R. J. C. Spreeuw, and J. P. Woerdman, "Orbital angular momentum of light and the transformation of Laguerre-Gaussian laser modes," Phys. Rev. A **45**(11), 8185–8189 (1992).
2. M. J. Padgett, "Orbital angular momentum 25 years on," Opt. Express **25**(10), 11265–11274 (2017).
3. C. Maurer, A. Jesacher, S. Bernet, and M. Ritsch-Marte, "What spatial light modulators can do for optical microscopy," Laser Photonics Rev. **5**(1), 81–101 (2011).
4. S. Fürhapter, A. Jesacher, S. Bernet, and M. Ritsch-Marte, "Spiral interferometry," Opt. Lett. **30**(15), 1953–1955 (2005).
5. A. E. Willner, H. Huang, Y. Yan, Y. Ren, N. Ahmed, G. Xie, C. Bao, L. Li, Y. Cao, Z. Zhao, J. Wang, M. P. J. Lavery, M. Tur, S. Ramachandran, A. F. Molisch, N. Ashrafi, and S. Ashrafi, "Optical communications using orbital angular momentum beams," Adv. Opt. Photonics **7**(1), 66–106 (2015).
6. D. L. Andrews, "Symmetry and quantum features in optical vortices," Symmetry **13**(8), 1368 (2021).
7. A. Alexandrescu, D. Cojoc, and E. D. Fabrizio, "Mechanism of angular momentum exchange between molecules and laguerre-gaussian beams," Phys. Rev. Lett. **96**(24), 243001 (2006).
8. M. Babiker, C. R. Bennett, D. L. Andrews, and L. C. Dávila Romero, "Orbital angular momentum exchange in the interaction of twisted light with molecules," Phys. Rev. Lett. **89**(14), 143601 (2002).
9. W. Löffler, D. J. Broer, and J. P. Woerdman, "Circular dichroism of cholesteric polymers and the orbital angular momentum of light," Phys. Rev. A **83**(6), 065801 (2011).
10. A. Picón, A. Benseny, J. Mompart, J. R. V. de Aldana, L. Plaja, G. F. Calvo, and L. Roso, "Transferring orbital and spin angular momenta of light to atoms," New J. Phys. **12**(8), 083053 (2010).
11. J. Lloyd-Hughes, P. M. Oppeneer, T. P. dos Santos, A. Schleife, S. Meng, M. A. Sentef, M. Ruggenthaler, A. Rubio, I. Radu, M. Murnane, X. Shi, H. Kapteyn, B. Stadtmüller, K. M. Dani, F. H. da Jornada, E. Prinz, M. Aeschlimann, R. L. Milot, M. Burdanova, J. Boland, T. Cocker, and F. Hegmann, "The 2021 ultrafast spectroscopic probes of condensed matter roadmap," J. Phys.: Condens. Matter **33**(35), 353001 (2021).
12. X. Shi, C.-T. Liao, Z. Tao, E. Cating-Subramanian, M. M. Murnane, C. Hernández-García, and H. C. Kapteyn, "Attosecond light science and its application for probing quantum materials," J. Phys. B: At., Mol. Opt. Phys. **53**(18), 184008 (2020).
13. J. Biegert, F. Calegari, N. Dudovich, F. Quéré, and M. Vrakking, "Attosecond technology(ies) and science," J. Phys. B: At., Mol. Opt. Phys. **54**(7), 070201 (2021).
14. J. S. Woods, X. M. Chen, R. V. Chopdekar, B. Farmer, C. Mazzoli, R. Koch, A. S. Tremsin, W. Hu, A. Scholl, S. Kevan, S. Wilkins, W.-K. Kwok, L. E. De Long, S. Roy, and J. T. Hastings, "Switchable x-ray orbital angular momentum from an artificial spin ice," Phys. Rev. Lett. **126**(11), 117201 (2021).
15. M. van Veenendaal and I. McNulty, "Prediction of strong dichroism induced by x rays carrying orbital momentum," Phys. Rev. Lett. **98**(15), 157401 (2007).
16. S. Patchkovskii and M. Spanner, "High harmonics with a twist," Nat. Phys. **8**(10), 707–708 (2012).
17. K. M. Dorney, L. Rego, N. J. Brooks, J. San Román, C.-T. Liao, J. L. Ellis, D. Zusin, C. Gentry, Q. L. Nguyen, J. M. Shaw, A. Picón, L. Plaja, H. C. Kapteyn, M. M. Murnane, and C. Hernández-García, "Controlling the polarization and vortex charge of attosecond high-harmonic beams via simultaneous spin–orbit momentum conservation," Nat. Photonics **13**(2), 123–130 (2019).
18. G. Gariepy, J. Leach, K. T. Kim, T. J. Hammond, E. Frumker, R. W. Boyd, and P. B. Corkum, "Creating high-harmonic beams with controlled orbital angular momentum," Phys. Rev. Lett. **113**(15), 153901 (2014).

Optics EXPRESS

19. C. Hernández-García, A. Picón, J. San Román, and L. Plaja, "Attosecond extreme ultraviolet vortices from high-order harmonic generation," Phys. Rev. Lett. **111**(8), 083602 (2013).
20. J. W. Wang, M. Zepf, and S. G. Rykovanov, "Intense attosecond pulses carrying orbital angular momentum using laser plasma interactions," Nat. Commun. **10**(1), 5554 (2019).
21. Y. Shen, X. Wang, Z. Xie, C. Min, X. Fu, Q. Liu, M. Gong, and X. Yuan, "Optical vortices 30 years on: Oam manipulation from topological charge to multiple singularities," Light: Sci. Appl. **8**(1), 90 (2019).
22. L. Rego, K. M. Dorney, N. J. Brooks, Q. L. Nguyen, C.-T. Liao, J. San Román, D. E. Couch, A. Liu, E. Pisanty, M. Lewenstein, L. Plaja, H. C. Kapteyn, H. C. Kapteyn, M. M. Murnane, and C. Hernández-García, "Generation of extreme-ultraviolet beams with time-varying orbital angular momentum," Science **364**(6447), eaaw9486 (2019).
23. E. Hemsing, A. Knyazik, M. Dunning, D. Xiang, A. Marinelli, C. Hast, and J. B. Rosenzweig, "Coherent optical vortices from relativistic electron beams," Nat. Phys. **9**(9), 549–553 (2013).
24. P. Rebernik Ribič, B. Rösner, D. Gauthier, E. Allaria, F. Döring, L. Foglia, L. Giannessi, N. Mahne, M. Manfredda, C. Masciovecchio, R. Mincigrucci, N. Mirian, E. Principi, E. Roussel, A. Simoncig, S. Spampinati, C. David, and G. De Ninno, "Extreme-ultraviolet vortices from a free-electron laser," Phys. Rev. X **7**(3), 031036 (2017).
25. J. Morgan, E. Hemsing, B. W. J. McNeil, and A. Yao, "Free electron laser generation of x-ray poincaré beams," New J. Phys. **22**(7), 072001 (2020).
26. E. L. Saldin, E. A. Schneidmiller, and M. V. Yurkov, "Optical afterburner for an x-ray free electron laser as a tool for pump-probe experiments," Phys. Rev. Spec. Top.–Accel. Beams **13**(3), 030701 (2010).
27. S. Sasaki, I. McNulty, and R. Dejus, "Undulator radiation carrying spin and orbital angular momentum," Nucl. Instrum. Methods Phys. Res., Sect. A **582**(1), 43–46 (2007).
28. S. Sasaki and I. McNulty, "Proposal for generating brilliant x-ray beams carrying orbital angular momentum," Phys. Rev. Lett. **100**(12), 124801 (2008).
29. E. Hemsing, M. Dunning, C. Hast, T. Raubenheimer, and D. Xiang, "First characterization of coherent optical vortices from harmonic undulator radiation," Phys. Rev. Lett. **113**(13), 134803 (2014).
30. P. R. Ribič, D. Gauthier, and G. De Ninno, "Generation of coherent extreme-ultraviolet radiation carrying orbital angular momentum," Phys. Rev. Lett. **112**(20), 203602 (2014).
31. E. A. Seddon, J. A. Clarke, D. J. Dunning, C. Masciovecchio, C. J. Milne, F. Parmigiani, D. Rugg, J. C. H. Spence, N. R. Thompson, K. Ueda, S. M. Vinko, J. S. Wark, and W. Wurth, "Short-wavelength free-electron laser sources and science: a review," Rep. Prog. Phys. **80**(11), 115901 (2017).
32. N. Huang, H. Deng, B. Liu, D. Wang, and Z. Zhao, "Features and futures of x-ray free-electron lasers," Innovation **2**(2), 100097 (2021).
33. E. Hemsing, "Coherent photons with angular momentum in a helical afterburner," Phys. Rev. Accel. Beams **23**(2), 020703 (2020).
34. D. J. Dunning, B. W. J. McNeil, and N. R. Thompson, "Few-cycle pulse generation in an x-ray free-electron laser," Phys. Rev. Lett. **110**(10), 104801 (2013).
35. R. Abela, A. Alarcon, and J. Alex, *et al.*, "The swissfel soft x-ray free-electron laser beamline: Athos," J. Synchrotron Radiat. **26**(4), 1073–1084 (2019).
36. G. Penco, G. Perosa, and E. Allaria, *et al.*, "Nonlinear harmonics of a seeded free-electron laser as a coherent and ultrafast probe to investigate matter at the water window and beyond," Phys. Rev. A **105**(5), 053524 (2019).
37. S. Ackermann, B. Faatz, V. Grattoni, M. M. Kazemi, T. Lang, C. Lechner, G. Paraskaki, J. Zemella, G. Geloni, S. Serkez, T. Tanikawa, and W. Hillert, "Novel method for the generation of stable radiation from free-electron lasers at high repetition rates," Phys. Rev. Accel. Beams **23**(7), 071302 (2020).
38. D. J. Dunning, N. R. Thompson, and B. W. J. McNeil, "Design study of an hhg-seeded harmonic cascade free-electron laser," J. Mod. Opt. **58**(16), 1362–1373 (2011).
39. L. T. Campbell and B. W. J. McNeil, "Puffin: A three dimensional, unaveraged free electron laser simulation code," Phys. Plasmas **19**(9), 093119 (2012).
40. L. T. Campbell, J. D. A. Smith, P. Traczykowski, and B. W. J. McNeil, "An updated description of the fel simulation code puffin," *9th International Particle Accelerator Conference* **IPAC2018, Vancouver, BC, Canada**, 4579–4582 (2018).
41. R. W. Schoenlein, "New Science Opportunities Enabled by LCLS-II X-ray Lasers," Tech. Rep. SLAC-R-1053, SLAC National Accelerator Laboratory (2015).
42. R. Bonifacio, L. De Salvo, P. Pierini, N. Piovella, and C. Pellegrini, "Spectrum, temporal structure, and fluctuations in a high-gain free-electron laser starting from noise," Phys. Rev. Lett. **73**(1), 70–73 (1994).
43. D. J. Dunning, B. W. J. McNeil, N. Thompson, and P. H. Williams, "Start-To-End Simulations of SASE and HHG-Seeded Mode-Locked FEL," in *Proc. FEL'09*, (JACoW Publishing, Geneva, Switzerland, 2009), pp. 165–168.
44. D. J. Dunning, B. W. J. McNeil, N. R. Thompson, and P. H. Williams, "Start-to-end modelling of a mode-locked optical klystron free electron laser amplifier," Phys. Plasmas **18**(7), 073104 (2011).
45. E. A. Schneidmiller and M. V. Yurkov, "Obtaining high degree of circular polarization at x-ray free electron lasers via a reverse undulator taper," Phys. Rev. Spec. Top.–Accel. Beams **16**(11), 110702 (2013).
46. J. P. MacArthur, A. A. Lutman, J. Krzywinski, and Z. Huang, "Microbunch rotation and coherent undulator radiation from a kicked electron beam," Phys. Rev. X **8**(4), 041036 (2018).
47. E. Ferrari, E. Roussel, J. Buck, C. Callegari, R. Cucini, G. De Ninno, B. Diviacco, D. Gauthier, L. Giannessi, L. Glaser, G. Hartmann, G. Penco, F. Scholz, J. Seltmann, I. Shevchuk, J. Viefhaus, M. Zangrando, and E. M. Allaria,

Optics EXPRESS

"Free electron laser polarization control with interfering crossed polarized fields," Phys. Rev. Spec. Top.–Accel. Beams **22**(8), 080701 (2019).
48. H. Deng, T. Zhang, L. Feng, C. Feng, B. Liu, X. Wang, T. Lan, G. Wang, W. Zhang, X. Liu, J. Chen, M. Zhang, G. Lin, M. Zhang, D. Wang, and Z. Zhao, "Polarization switching demonstration using crossed-planar undulators in a seeded free-electron laser," Phys. Rev. Spec. Top.–Accel. Beams **17**(2), 020704 (2014).
49. S. Serkez, A. Trebushinin, M. Veremchuk, and G. Geloni, "Method for polarization shaping at free-electron lasers," Phys. Rev. Accel. Beams **22**(11), 110705 (2019).
50. J. Morgan and B. W. J. McNeil, "Attosecond polarization modulation of x-ray radiation in a free-electron laser," Phys. Rev. Accel. Beams **24**(1), 010701 (2021).
51. N. Sudar, R. Coffee, and E. Hemsing, "Coherent x rays with tunable time-dependent polarization," Phys. Rev. Accel. Beams **23**(12), 120701 (2020).